MEK/ERK and PI3K/AKT pathway inhibitors affect the transformation of myelodysplastic syndrome into acute myeloid leukemia via H3K27me3 methylases and de-methylases

ZHUANZHEN ZHENG, XIUHUA CHEN, YAOFANG ZHANG, FANGGANG REN and YANPING MA

Department of Hematopathology, Second Hospital of Shanxi Medical University, Taiyuan, Shanxi 030001, P.R. China

Received December 22, 2022; Accepted July 28, 2023

DOI: 10.3892/ijo.2023.5588

Abstract. The transformation of myelodysplastic syndrome (MDS) into acute myeloid leukemia (AML) poses a significant clinical challenge. The trimethylation of H3 on lysine 27 (H3K27me3) methylase and de-methylase pathway is involved in the regulation of MDS progression. The present study investigated the functional mechanisms of the MEK/ERK and PI3K/AKT pathways in the MDS-to-AML transformation. MDS-AML mouse and SKM-1 cell models were first established and this was followed by treatment with the MEK/ERK pathway inhibitor, U0126, the PI3K/AKT pathway inhibitor, Ly294002, or their combination. H3K27me3 methylase, enhancer of zeste homolog (EZH)1, EZH2, demethylase Jumonji domain-containing protein-3 (JMJD3) and ubiquitously transcribed tetratricopeptide repeat on chromosome X (UTX) and H3K27me3 protein levels were determined using western blot analysis. Cell viability, cycle distribution and proliferation were assessed using CCK-8, flow cytometry, EdU and colony formation assays. The ERK and AKT phosphorylation levels in clinical samples and established models were determined, and SKM-1 cell behaviors were assessed. The levels of H3K27me3 methylases and de-methylases and distal-less homeobox 5 (DLX5) were measured. The results revealed that the ERK and AKT phosphorylation levels were elevated in patients with MDS and MDS-AML, and in mouse models. Treatment with U0126, a MEK/ERK pathway inhibitor, and Ly294002, a PI3K/AKT pathway inhibitor, effectively suppressed ERK and AKT phosphorylation in mice with MDS-AML. It was observed that mice with MDS treated with U0126/Ly294002 exhibited reduced transformation to AML, delayed disease transformation and increased survival rates. Treatment of the SKM-1 cells with U0126/Ly294002 led to a decrease in cell viability and proliferation, and to an increase in cell cycle arrest by suppressing ERK/PI3K phosphorylation. Moreover, treatment with U0126/Ly294002 downregulated EZH2/EZH1 expression, and upregulated JMJD3/UTX expression. The effects of U0126/Ly294002 were nullified when EZH2/EZH1 was overexpressed or when JMJD3/UTX was inhibited in the SKM-1 cells. Treatment with U0126/Ly294002 also resulted in a decreased H3K27me3 protein level and H3K27me3 level in the DLX5 promoter region, leading to an increased DLX5 expression. Overall, the findings of the present study suggest that U0126/Ly294002 participates in MDS-AML transformation by modulating the levels of H3K27me3 methylases and de-methylases, and regulating DLX5 transcription and expression.

Correspondence to: Dr Yanping Ma, Department of Hematopathology, Second Hospital of Shanxi Medical University, 382 Wuyi Road, Xinghualing, Taiyuan, Shanxi 030001, P.R. China
E-mail: myanping0607@163.com

Key words: myelodysplastic syndrome, acute myeloid leukemia, SKM-1 cells, MEK/ERK, PI3K/AKT, U0126, Ly294002, H3K27me3, distal-less homeobox 5

Introduction

Myelodysplastic syndrome (MDS) is a heterogeneous group of bone marrow disorders characterized by ineffective and dysplastic hematopoiesis, peripheral blood cytopenias and a high risk for transformation into acute myeloid leukemia (AML) (1-3). MDS is considered a type of malignant neoplasm of the blood system and is genetically associated with AML, with ~30% of patients with MDS eventually developing AML (4). MDS is caused by abnormal bone marrow hematopoietic stem cell function, bone marrow microenvironmental changes, genetic or chromosomal abnormalities, and epigenetic abnormalities (5-7). While the transformation of MDS into AML has been hypothesized to result from a single genetic or epigenetic event (8), the exact mechanisms behind the MDS initiation, progression and transformation into AML are not yet fully understood.

The mitogen extracellular kinase (MEK)/extracellular signal-regulatedkinase(ERK)andphosphatidylinositol-3-kinase (PI3K)/serine-threonine protein kinase (AKT) pathways have been identified as central signaling pathways in numerous types of cancer, closely associated with cellular proliferation, invasion and metastasis (9-11). It has also been suggested that these pathways may contribute to the transformation of MDS into AML (12,13). In particular, targeting these pathways has emerged as a potential therapeutic strategy for Ras-driven malignancies, such as MDS (14,15). Notably, the activation of the MEK/ERK pathway has been shown to play a critical role in the transformation of hematopoietic cells, emphasizing its

potential as a therapeutic target for MDS (14,15). Therefore, it was hypothesized that targeting the MEK/ERK and PI3K/AKT pathways may be a promising approach for the treatment of MDS and preventing its transformation into AML.

Histone modifications, particularly methylation, play a pivotal role in gene expression regulation and the pathogenesis of MDS (7,16). Histone methylation represents one of the most significant epigenetic mechanisms (17). Specifically, the histone lysine methyltransferases, enhancer of zeste homolog 1/2 (EZH1/2), and the de-methylases, ubiquitously transcribed tetratricopeptide repeat on chromosome X (UTX) and Jumonji domain-containing protein 3 (JMJD3), are involved in histone H3 lysine 27 (H3K27) methylation and de-methylation (18). Previous research has reported that EZH2 activity is repressed upon the inhibition of the PI3K/AKT pathway in myeloma cells, and the upregulation of EZH1 partly compensates for the loss of EZH2 activity (19). Additionally, ERK and AKT pathway suppression in metastatic colon cancer cells has been shown to result in a decreased expression of EZH2 (20). Based on these findings, it was hypothesized that the MEK/ERK and PI3K/AKT pathways may contribute to MDS progression and transformation into AML by modulating histone methylation via the H3K27me3 level and associated methylases and de-methylases.

Additionally, the association between the distal-less homeobox 5 (DLX5) gene and MDS-AML transformation has been established, with DLX5 exhibiting antitumor properties in both AML and MDS (21). However, the histone modifiers, EZH2 and EHMT2, have been found to inhibit DLX5 transcription through H3K27me3 and H3K9me2 catalysis, respectively, facilitating MDS-AML transformation (22). Therefore, it was hypothesized that MEK/ERK and PI3K/AKT pathway inhibitors may regulate DLX5 transcription via H3K27me3 methylation/de-methylation, thus manipulating MDS-AML transformation. The present study aimed to elucidate the mechanisms of action of the MEK/ERK and PI3K/AKT pathways in the MDS-AML transformation, as well as to provide new evidence for the potential of these pathways as therapeutic targets in MDS, where there is currently a lack of documentation regarding this hypothesis.

Materials and methods

Ethics statements. The present study was conducted in accordance with the guidelines of the Ethics Committee of Second Hospital of Shanxi Medical University (Taiyuan, China). Informed consent was obtained from all participants before sampling (Approval no. 2020-YX-056). The animal experiments were performed with the aim of minimizing the number of animals used and reducing their suffering (Approval no. 2020-K52).

Patients and specimens. Bone marrow samples were collected from 45 patients between 2020 and 2021 via bone marrow puncture and/or biopsy. These included specimens from patients diagnosed with MDS (n=15), MDS-AML (n=15) and cancer-free individuals (normal group, n=15). MDS-AML specimens were obtained from patients who initially presented with MDS and subsequently progressed to AML. Age and sex were matched between the patients with MDS and MDS-AML. There were no significant differences in age, sex and body mass index (BMI) among the three groups (all P>0.05; Table I). The samples were separated using human peripheral blood lymphocyte separation solution (TBD, https://www.tbdscience.com) via the density gradient method. Western blot analysis was used to determine the expression levels of the MEK/ERK and PI3K/AKT pathways.

Patient inclusion and exclusion criteria. The inclusion criteria were as follows: i) Patients were confirmed by morphological, immunological and cytogenetics examinations of myelocytes to meet the relevant diagnostic criteria for MDS and MDS-AML according to the WHO classification of hematopoietic and lymphoid tissue tumors (23); ii) an age >18 years; iii) patients signed an informed consent form. The exclusion criteria were the following: i) Patients also had other malignant tumors concomitantly; ii) patients with severe liver and kidney dysfunctions; iii) patients with coagulation disorders; iv) patients with infectious diseases; and v) patients with concomitant autoimmune diseases.

Experimental animals. A total of 12 male C57BL/6 mice (3 weeks old, weighing 11.5±1.2 g) [Chengdu Dossy Experimental Animals, SCXK(Chuan)2019-028] and 60 male NHD13 mice (3 weeks old, weighing 10.2±1.3 g) (Jackson Laboratory) were housed in a specific pathogen-free animal facility and provided with free access to food and drinking water. Following 1 week of acclimatization, all mice (4 weeks old) were divided into six groups as follows (n=12 per group): i) The C57BL/6 group; ii) NHD13 group; iii) NHD13 + dimethyl sulfoxide (DMSO) group (NHD13 mice were intraperitoneally injected with 0.3% DMSO (0.2 ml) as the solvent control for U0126 or Ly294002); iv) NHD13 + U0126 group (NHD13 mice were intraperitoneally injected with the MEK/ERK pathway inhibitor, U0126 at 10 mg/kg/day); v) NHD13 + Ly294002 group (NHD13 mice were intraperitoneally injected with the PI3K/AKT pathway inhibitor, Ly294002, at 10 mg/kg/day); and vi) the NHD13 + U0126 + Ly294002 group (NHD13 mice were intraperitoneally injected with U0126 and Ly294002 at 10 mg/kg/day). U0126 and Ly294002 were supplied by MedChemExpress, dissolved in DMSO and diluted with normal saline. The administration and dosage of U0126 and Ly294002 were based on previous studies (24,25), the manufacturer's protocol and a pre-experiment (in the pre-experiment, U0126 or Ly294002 at concentrations of 1 and 10 mg/kg/day were selected for treatment of the NHD13 mice for 2 months; U0126 or Ly294002 at concentrations of 10 mg/kg/day had a more prominent therapeutic effect; Data S1 and Fig. S1). Following 2 months of consecutive treatment, the mice were anesthetized with ether, and 0.2 ml peripheral blood samples were collected from the orbital venous plexus of each mouse (n=6 mice per group) to count the number of peripheral white blood cells (WBCs), red blood cells (RBCs) and platelets (PLTs) using an automatic animal blood cell analyzer BC2800Vet (Mindray), and the phosphorylation levels of ERK and AKT were measured using western blot analysis. Peripheral blood samples were then

Table I. General information of the study participants.

Characteristic	Normal (n=15)	MDS (n=15)	MDS-AML (n=15)	P-value
Age (years)	49.5±11.2	48.9±12.4	49.3±12.6	0.9905
Sex (male/female)	7/8	7/8	8/7	0.9149
BMI (kg/m^2)	22.6±1.31	22.8±1.53	22.5±1.37	0.8384

BMI, body mass index; MDS, myelodysplastic syndrome; AML, acute myeloid leukemia. Age and BMI are continuous variables and are expressed as the mean ± standard deviation. Multi-group comparisons were performed using one-way analysis of variance with Tukey's post hoc test. Sex is a categorical variable and is expressed as the number of cases. Multi-group comparisons were performed using the Chi-squared test. There were no significant differences in age, sex and BMI among the normal, MDS and MDS-AML groups (all P>0.05).

collected every 2 weeks to monitor the MDS to AML transformation in the NHD13 mice. AML was defined by the presence of myeloblasts ≥20% in peripheral blood (26,27). At 14 months (420 days), all mice were euthanized by an intraperitoneal injection of pentobarbital sodium (800 mg/kg) (22,28) after the final blood collection.

Cells, cell culture and cell grouping. The human MSD/AML cell line, SKM-1 (cat. no. 151 BNCC341806, BeNa Culture Collection), was cultured in RPMI-1640 medium containing 10% fetal bovine serum at 37˚C in a 5% CO_2 and 95% humidified air incubator. The SKM-1 cells at the exponential phase were seeded in 12-well plates at a density of 1x10^5 cells/well and the following groups were established: i) The SKM-1 group, SKM-1 + DMSO group, SKM-1 + U0126 group, SKM-1 + Ly294002 group, and SKM-1 + U0126 + Ly294002 group (the SKM-1 group did not receive any treatment, the SKM-1 + DMSO group was a solvent control group with an equal amount of DMSO added, and the other groups were treated with U0126 and Ly294002 alone or in combination for 48 h, respectively); ii) the U0126 + oe-negative control (NC) group and U0126 + oe-EZH2 group [transfected with EZH2 overexpression plasmid (oe-EZH2) or control plasmid (oe-NC) for 48 h, followed by U0126 treatment for 48 h]; iii) U0126 + si-NC group and U0126 + si-JMJD3 group [transfected with small interfering RNA (siRNA; si-JMJD3) or negative control (si-NC) of JMJD3 for 48 h, followed U0126 treatment for 48 h]; iv) Ly294002 + oe-NC group and Ly294002 + oe-EZH1 group (transfected with oe-EZH1 or oe-NC for 48 h, followed by Ly294002 treatment for 48 h); v) Ly294002 + si-NC group and Ly294002 + si-UTX group (transfected with si-UTX or si-NC for 48 h, followed by Ly294002 treatment for 48 h). DMSO was used as the solvent for both U0126 and Ly294002. The concentrations of U0126 and Ly294002 (both 5 μM) were referred to in the literature (24,29) and the pre-experiment (Data S1 and Fig. S2). The plasmids, oe-EZH1, si-JMJD3 and oe-EZH2 and si-UTX, as well as their negative controls were designed and synthesized by GenePharma Co., Ltd. The dose of plasmid was 500 ng/well, and the dose of siRNA was 150 ng/well. The sequences of the siRNAs used were as follows: si-NC, 5'-UUCUCCGAACGUGUCACGUTT-3'; si-JMJD3, 5'-GCUACACCUUGAGCACAAATdT-3'; si-UTX, 5'-GGACUUGCAGCACGAAUUATT-3'. Transfection was performed at 37˚C for 24 h using Lipofectamine 2000® (Invitrogen; Thermo Fisher Scientific, Inc.), followed by subsequent experiments 48 h later.

Cell Counting Kit-8 (CCK-8) assay. As previously reported (30), SKM-1 cells in the logarithmic phase or SKM-1 cells (5x10^3/well) following transfection were seeded in 96-well plates and grouped as previously described. The viability of the SKM-1 cells at 24, 48 and 72 h was assessed using CCK-8 assay (cat. no. C0038, Beyotime Institute of Biotechnology). Subsequently, the SKM-1 cells in the 96-well plates were incubated with 100 μl CCK-8 solution at 37˚C for 4 h, and the absorbance at 450 nm (OD450) was measured using the Multiskan SkyHigh Microplate Spectrophotometer (Thermo Scientific™ SkanIt Software, Thermo Fisher Scientific, Inc.). A total of three independent experiments were performed for each group.

Flow cytometry. The SKM-1 cells were fixed in 70% ethanol at 4˚C overnight, stained with 300 ml propidium iodide (Hangzhou Multi Sciences (Lianke) Biotech Co., Ltd.) in the dark at 37˚C for 30 min, and subsequently analyzed for cell cycle distribution using a flow cytometer (MoFloAstrios EQ, Beckman Coulter) with FlowJo V10.8.1 software (Leonard Herzenberg Laboratory, Stanford University, USA), as previously described (30).

5-Ethynyl-2'-deoxyuridine (EdU) assay. The SKM-1 cells were rinsed with phosphate-buffered saline (PBS) after removing the culture medium, and then incubated with 100 μl EdU staining solution (cat. no. CA1170-100T, Shanghai Acmec Biochemical Co., Ltd.) for 2 h. Following 1-2 rinses with PBS, the cells were fixed with 50 μl 4% paraformaldehyde at room temperature for 30 min, followed by washing with PBS and incubation with 100 μl 0.5% Triton X-100 (cat. no. HFH10, Invitrogen; Thermo Fisher Scientific, Inc.) at room temperature for 10 min. The cells were then washed with PBS, stained with 100 μl Apollo staining solution (cat. no. CA1170-100T, Shanghai Acmec Biochemical Technology Co., Ltd.) in the dark at room temperature for 30 min, and then subjected to PBS washing and incubation with 100 μl 0.5% TritonX-100 at room temperature for 10 min. After rinsing with PBS, the cells were incubated with DAPI staining solution (cat. no. D1306, Invitrogen; Thermo Fisher Scientific, Inc.) at room temperature in the dark for 30 min, and then rinsed with PBS. Subsequently, a

Table II. Sequences of primers used in RT-qPCR.

Gene	Primer sequence
GAPDH	F: 5'-GGGAGCCAAAAGGGTCAT-3'
	R: 5'-GAGTCCTTCCACGATACCAA-3'
DLX5	F: 5'-ATGACAGGAGTGTTTGACAGAAG-3'
	R: 5'-CTAATAGAGTGTCCCGGAGGCCA-3'
DLX5 ChIP primer 1	F: 5'-TTCTACACTCGCCTTTGGTG-3'
	R: 5'-CAGCACAAGGCTCTGTGATG-3'
DLX5 ChIP primer 2	F: 5'-CCCACTCCACAACAAGCAA-3'
	R: 5'-GCACAGCCTTGGTTAAATCC-3'

RT-qPCR, reverse transcription-quantitative polymerase chain reaction; GAPDH, glyceraldehyde-3-phosphate dehydrogenase; DLX5, distal-less homeobox gene 5; ChIP, chromatin immunoprecipitation; F, forward; R, reverse.

fluorescence microscope (Olympus Corporation) was used for observation and imaging, as previously described (31).

Colony formation assay. The SKM-1 cells were seeded in 12-well plates at a density of $1x10^4$ cells/well and cultured at 37˚C for 1 week until colony formation was visible. After rinsing with PBS, the cells were fixed with 500 μl 4% paraformaldehyde (cat. no. R37814, Invitrogen; Thermo Fisher Scientific, Inc.) at 37˚C for 60 min, washed with PBS, and stained with 0.1% crystal violet solution (cat. no. YT8810; Yita Biotech) at 37˚C for 30 min. The colonies were then observed and counted under a light microscope (BX53; Olympus Corporation), as previously described (31).

Chromatin immunoprecipitation (ChIP). ChIP was conducted using a kit (Diagenode Diagnostics) on the STAR compact automation system, as previously described (32). The SKM-1 cells were counted using a handheld automated cell counter based on the Coulter principle (Scepter 2.0, MilliporeSigma) following detachment with trypsin. For each treatment, ~$1x10^4$ cells were used. The cells were fixed with formaldehyde for 8 min at room temperature and cross-linked for 5 min using 1.25 M glycine (cat. no. G7126, MilliporeSigma) at room temperature. Chromatin was then fragmented into 500 bp by ultrasound treatment, followed by ChIP at 4˚C. The cross-linked cells were rinsed with PBS inhibitor solution (NaBu, 20 mM; cat. no. B5887, MilliporeSigma) and the cell membranes were lysed using the HighCell ChIP kit (cat. no. C01010062, Diagenode). Chromatin was then prepared in TPX tubes with shearing buffer S1 and 1X protease inhibitor and then fragmented again into 500 bp by ultrasound. The fragment size was assessed on a 2% agarose gel, and the sheared chromatin was preserved at -80˚C. DNA was immunoprecipitated using 2 μg anti-H3K27me3 antibody (10 μg for 25 μg chromatin, cat. no. ab6002, Abcam) or non-immune IgG (2 μg, cat. no. ab171870, Abcam), and purified using DNA isolation buffer following the instructions provided with the HighCell ChIP kit. Each Auto-ChIP sample was prepared using the Auto Histone ChIP-seq kit, and 1 μg input chromatin was included. The reaction was incubated for 2 h for the antibody with protein A-coated magnetic beads, followed by 10 h of immunoprecipitation at 4˚C and centrifugation at 4˚C and 1,000 x g for 30 sec, and the supernatant was removed. The precipitate was washed with 500 μl low-salt wash buffer, high-salt wash buffer, LiCl wash buffer and TE buffer, respectively and centrifuged at 1,000 x g and 4˚C for 30 sec; this was followed by the addition of 500 μl eluent (100 μl 10% SDS, 100 μl 1 M $NaHCO_3$, 800 μl ddH_2O, a total of 1 ml), shaking upside down at room temperature for 15 min, and was then allowed to stand for 10 min, and centrifuged at 4˚C and 1,000 x g for 1 min. The centrifugation tube was supplemented with 20 μl 5 M NaCl, mixed well with the samples, and then de-cross-linked at 65˚C overnight. The DNA samples from immunoprecipitation were recovered, and immunoprecipitated DNA (IP DNA) or total DNA Input, along with 1X SYBR-Green Supermix (Applied Biosystems; Thermo Fisher Scientific, Inc.) and the TSH2B promoter (pp-1041-500, Diagenode; positive control for methylation), were used for reverse transcription-quantitative polymerase chain reaction (RT-qPCR) to detect the binding, with the DLX5 promoter region sequence as the primer (Table II).

RT-qPCR. Total RNA was extracted from differently treated cells using the single-step method with TRIzol® reagent (Invitrogen; Thermo Fisher Scientific, Inc.), as previously described (30). High-quality RNA was verified by UV analysis and formaldehyde denaturing gel electrophoresis. Following the instructions provided with the reverse transcription kit (code no. FSQ-201, Toyobo Life Science), cDNA was synthesized, and the RT-qPCR kit (cat. no. F410L, Thermo Fisher Scientific, Inc.) was used for fluorescence qPCR on an ABI 7500-type RT fluorescence qPCR system (Applied Biosystems; Thermo Fisher Scientific, Inc.). The process included pre-denaturation at 94˚C for 2 min, and 35 cycles of denaturation at 94˚C for 30 sec, annealing at 55˚C for 30 sec, and extension at 72˚C for 1 min. PCR primers were designed and synthesized by Sangon Biotech Co., Ltd. (Table II). Relative expression was calculated using the $2^{-\Delta\Delta Cq}$ method with GAPDH as the internal reference (33).

Western blot analysis. The cells were lysed in a cold radioimmunoprecipitation assay lysis solution [Beijing Solarbio Science & Technology Co., Ltd.; main components: 50 mM Tris (pH 7.4), 150 mM NaCl, 1% TritonX-100, 1% sodium

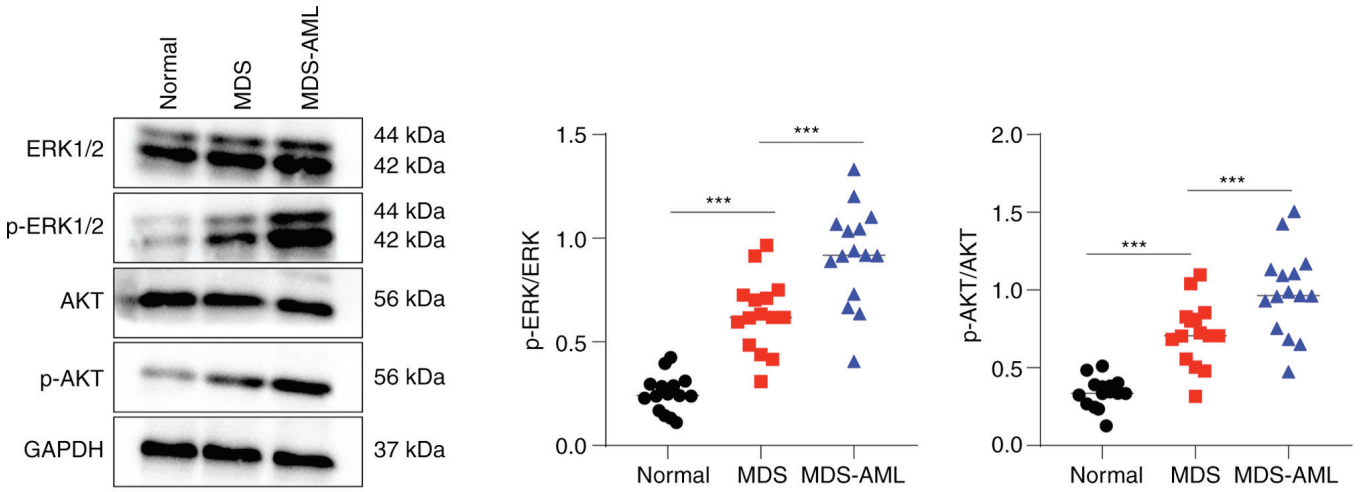

Figure 1. Abnormal activation of the MEK/ERK and PI3K/AKT pathways in patients with MDS and MDS-AML. Western blot analysis was performed to determine the phosphorylation levels of ERK and AKT in bone marrow samples of patients with MDS and MDS-AML and cancer-free individuals. Multi-group comparisons were performed using one-way ANOVA, followed by Tukey's multiple comparisons test. ***P<0.001. MDS, myelodysplastic syndrome; AML, acute myeloid leukemia.

deoxycholate, 0.1% SDS, and 2 mM sodium pyrophosphate, 25 mM β-glycerophosphate, 1 mM EDTA, 1 mM Na_3VO_4, 0.5 μg/ml leupeptin] supplemented with protease inhibitor mixture (MilliporeSigma) for 30 min, as previously reported (31). Following centrifugation at 16,000 x g for 30 min at 4˚C, the supernatant was collected. The protein concentration was determined using bicinchoninic acid protein detection kits (cat. no. P0012S, Beyotime Institute of Biotechnology). The 30 μg obtained protein lysate was separated by 10% SDS-PAGE, transferred onto PVDF membranes (MilliporeSigma), and blocked with 5% non-fat milk at room temperature for 2 h. The membranes were incubated overnight at 4˚C with primary antibodies, followed by incubation with HRP-coupled IgG H&L (1:2,000, cat. no. ab6721, Abcam) secondary antibody at room temperature for 1 h. The protein bands were visualized using chemiluminescence reagent and Gel Dol EZ Imager (Bio-Rad Laboratories, Inc.), and the gray value of the target protein band was analyzed using ImageJ V1.8.0 software (Institutes of Health). The primary antibodies used and their concentrations were as follows: ERK (1:10,000, cat. no. ab184699), p-ERK (1:1,000, cat. no. ab214036), AKT (1:1,000, cat. no. ab238477), p-AKT (1:1,000, cat. no. ab183556), EZH1 (1:1,000, cat. no. ab289887), EZH2 (1:1,000, cat. no. ab150433), JMJD3 (1 μg/ml, cat. no. ab169197), UTX (1:1,000, cat. no. ab300513), H3K27me3 (1:1,000, cat. no. ab6002), DLX5 (1:5,000, cat. no. ab109737) and GAPDH (1:2,500, cat. no. ab9485) (all from Abcam).

Statistical analysis. Statistical analyses were performed using SPSS 21.0 (IBM Corp.). Cell experiments were conducted in triplicate and animal experiments involved 6 mice per group. Categorical variables are presented as frequencies (number, n), and multi-group comparisons were assessed using the Chi-squared (χ^2) test. Continuous variables were assessed for normality using the Shapiro-Wilk test, and are presented as the mean ± standard deviation. Pairwise comparisons were performed using independent sample t-tests, while multi-group comparisons were made using one-way analysis of variance (ANOVA) with Tukey's post hoc test. Kaplan-Meier curves were used to analyze MDS-AML transformation and mouse survival, and differences were analyzed using the log-rank test. All P-values were two-tailed, and P<0.05 was considered to indicate a statistically significant difference.

Results

Activation of MEK/ERK and PI3K/AKT pathways in patients with MDS and MDS-AML. The phosphorylation levels of ERK and AKT in bone marrow specimens from the normal, MDS and MDS-AML groups were assessed using western blot analysis. The results revealed that the patients with MDS had significantly higher levels of p-ERK and p-AKT than the healthy volunteers, whereas the patients with MDS-AML exhibited significantly higher levels of p-ERK and p-AKT compared with the patients with MDS (all P<0.05, Fig. 1). These findings indicate the abnormal activation of the MEK/ERK and PI3K/AKT pathways in patients with MDS and MDS-AML.

Inhibition of MEK/ERK and PI3K/AKT pathways attenuates MDS-AML transformation in mice. The peripheral blood samples of normal C57BL/6 and NHD13 mice at the age of 3 months were collected to count the number of RBCs, WBCs and PLTs. The results revealed a significant decrease in in these parameters in the peripheral blood of NHD13 mice compared to the normal C57BL/6 mice (all P<0.05, Fig. 2A-C). Western blot analysis revealed a substantial increase in the phosphorylation levels of ERK and AKT in the NHD13 mice, indicating the abnormal activation of the MEK/ERK and PI3K/AKT pathways (all P<0.05, Fig. 2D).

Following treatment of the NHD13 mice with the MEK/ERK or/and PI3K/AKT pathway inhibitors, U0126 and Ly294002, respectively for 2 months, a significant increase in RBCs, WBCs, and PLTs in peripheral blood was observed, with combined treatment with U0126 and Ly294002 exhibiting the most favorable efficacy (all P<0.05, Fig. 2A-C). Western

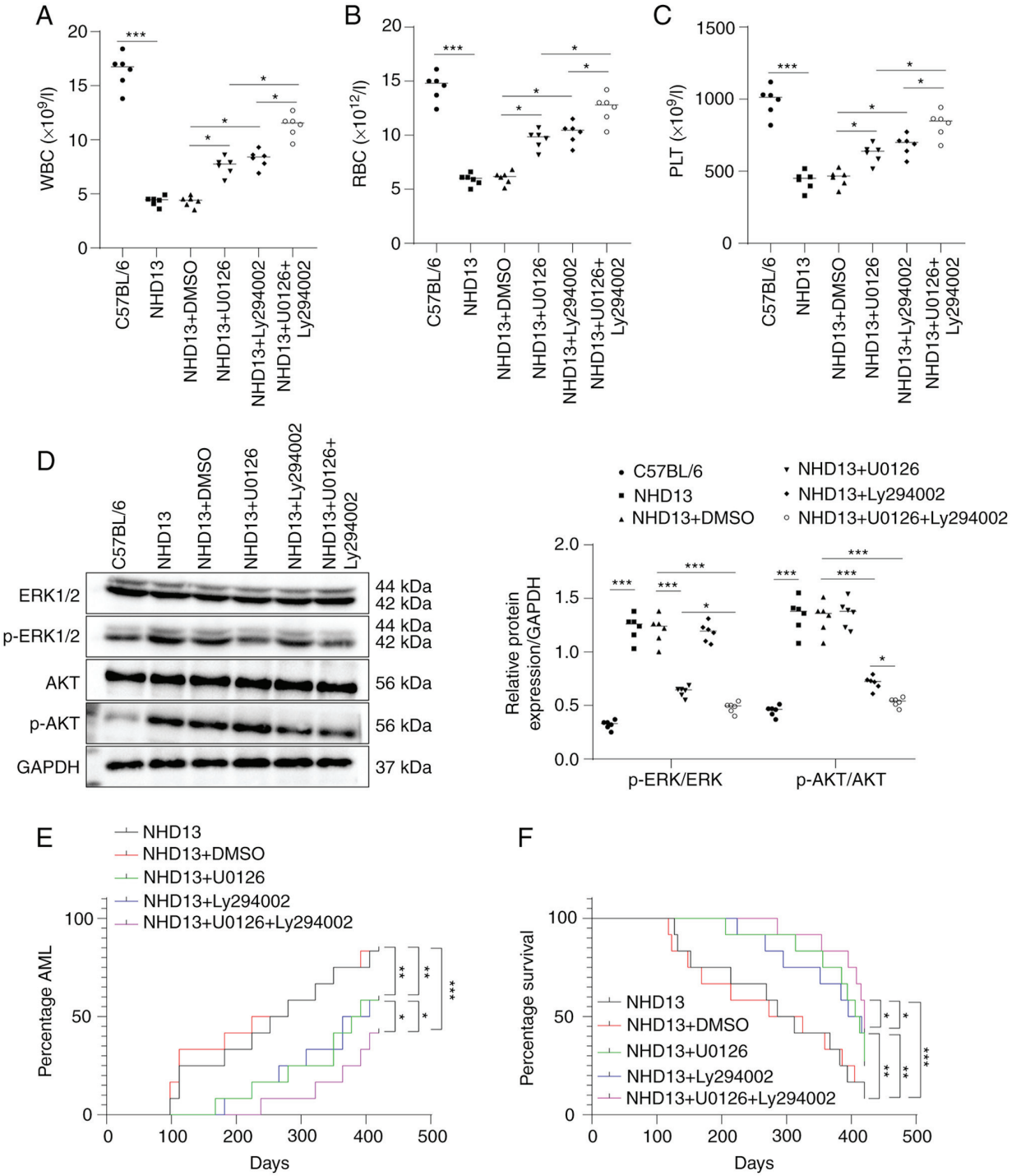

Figure 2. MEK/ERK and PI3K/AKT pathway inhibitors attenuate the MDS-AML transformation in NHD13 mice. (A-C) The numbers of WBCs, RBCs and PLTs in C57B/L6 mice or NHD13 mice in the different groups were counted using a full-automatic blood cell analyzer. (D) The protein levels of ERK, p-ERK, AKT and p-AKT in the peripheral blood of C57B/L6 mice or NHD13 mice in the different groups were determined using western blot analysis. (E) The numbers of NHD13 mice in which MDS transformed to AML within 14 months (420 days) and the transformation time. (F) The survival rates of NHD13 mice were analyzed using Kaplan-Meier survival curves. (A-D) n=6; multi-group comparisons were performed using one-way ANOVA, followed by Tukey's multiple comparisons test. *P<0.05, **P<0.01 and ***P<0.001. (E and F) n=12; comparisons between groups were performed using the log-rank test. p-, phosphorylated; MDS, myelodysplastic syndrome; AML, acute myeloid leukemia; WBC, white blood cells; RBC, red blood cell; PLT, platelet.

blot analysis indicated that treatment with U0126 suppressed ERK phosphorylation, while treatment with Ly294002 inhibited AKT phosphorylation in the NHD13 mice. Combined treatment with U0126 and Ly294002 led to more prominent inhibitory effects on the phosphorylation of ERK and AKT (all P<0.05, Fig. 2D).

Moreover, both U0126 and Ly294002 reduced the number of NHD13 mice undergoing the MDS-AML transformation and delayed the transformation time within 14 months (420 days), while the effects of U0126 in combination with Ly294002 were superior (all P<0.05, Fig. 2E). The Kaplan-Meier survival curve demonstrated an upward trend in NHD13 mouse survival

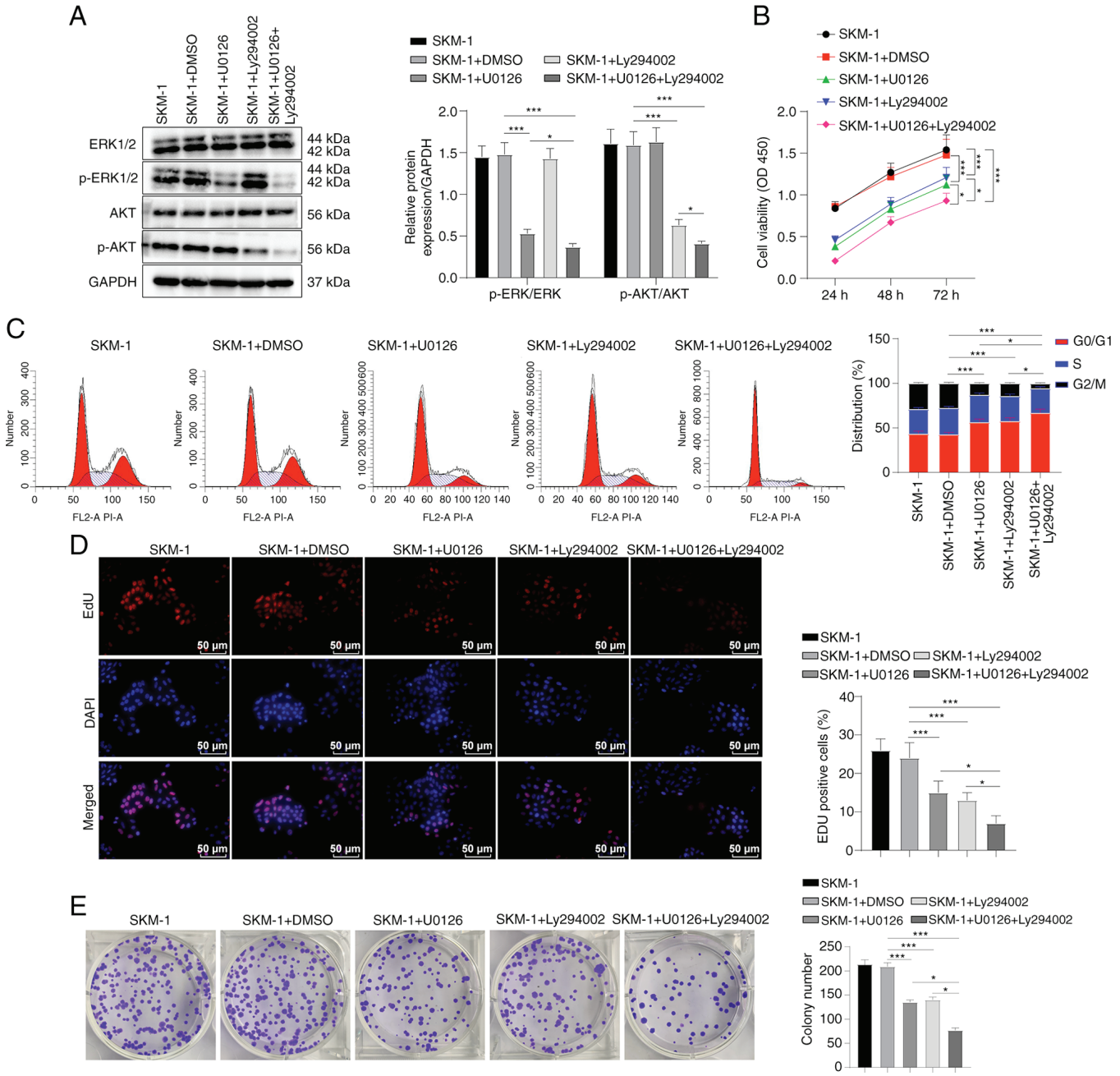

Figure 3. MEK/ERK and PI3K/AKT pathway inhibitors regulate the SKM-1 cell cycle and proliferation. (A) Western blot analysis was performed to determine the protein levels of ERK, p-ERK, AKT and p-AKT in SKM-1 cells. (B) SKM-1 cell viability was assessed using CCK-8 assay. (C) SKM-1 cell cycle progression was evaluated using flow cytometry. (D and E) SKM-1 cell proliferation was assessed using EdU and colony formation assays. Each cell experiment was repeated three times. The results are expressed as the mean ± standard deviation. Multi-group comparisons were performed using one-way ANOVA, followed by Tukey's multiple comparisons test. *P<0.05 and ***P<0.001.

after U0126 and Ly294002 treatment, and the survival rates were further increased after the combined treatment of U0126 and Ly294002 (Fig. 2F, all P<0.05). On the whole, these findings suggest that the MEK/ERK inhibitor, U0126, and the PI3K/AKT pathway inhibitor, Ly294002, attenuated the transformation of MDS into AML in NHD13 mice.

MEK/ERK and PI3K/AKT pathway inhibitors regulate the cell cycle progression and proliferation of SKM-1 cells. To investigate the effects of the MEK/ERK and PI3K/AKT pathway inhibitors on SKM-1 cells, an *in vitro* experiment was conducted in which the SKM-1 cells were treated with U0126 and Ly294002 either alone or in combination. Western blot analysis revealed that treatment with U0126 reduced the phosphorylation level of ERK, while treatment with Ly294002 reduced the phosphorylation level of AKT. Treatment with both U0126 and Ly294002 resulted in a significant decrease in the phosphorylation levels of ERK and AKT, with a more potent inhibitory effect compared to either inhibitor alone (all P<0.05, Fig. 3A).

The results of CCK-8 assay revealed that U0126 or Ly294002 inhibited SKM-1 cell viability, and the combination of both inhibitors exerted a more prominent inhibitory effect (all P<0.05, Fig. 3B). Flow cytometry demonstrated that

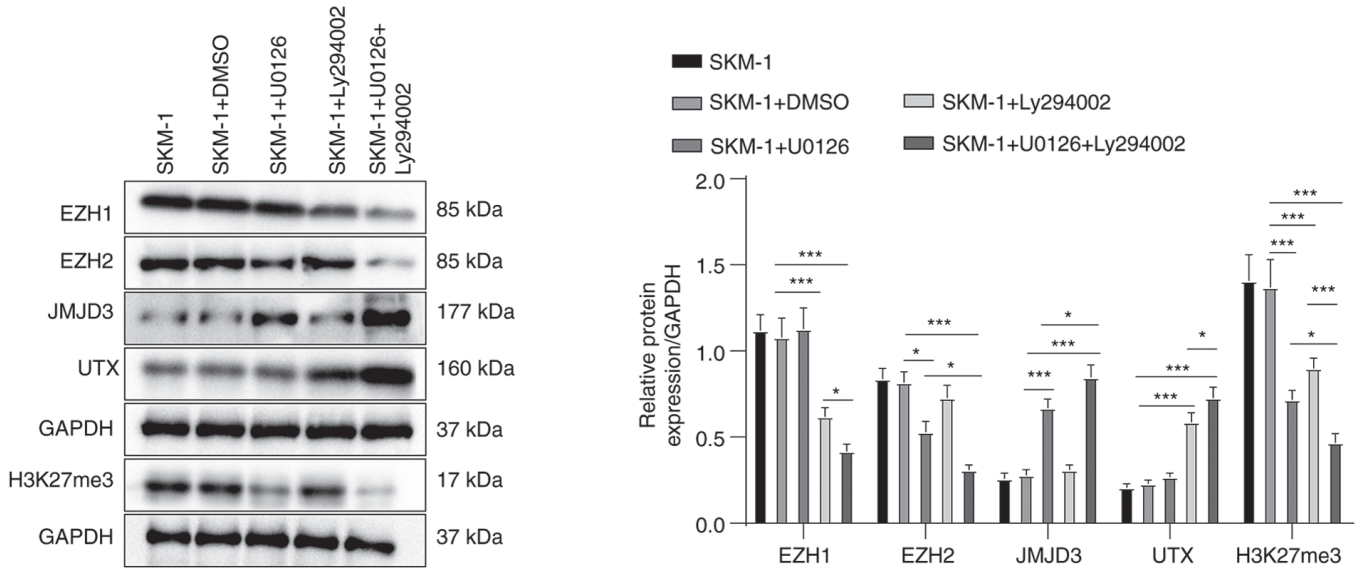

Figure 4. MEK/ERK and PI3K/AKT pathway inhibitors modulate the expression levels of H3K27me3 methylases and de-methylases. Western blot analysis was performed to determine the protein levels of H3K27me3 methylases EZH1, EZH2, and de-methylases JMJD3 and UTX, and H3K27me3 in SKM-1 cells. Each cell experiment was repeated three times. The results are expressed as the mean ± standard deviation. Multi-group comparisons were performed using one-way ANOVA, followed by Tukey's multiple comparisons test. *P<0.05 and ***P<0.001. H3K27me3, trimethylation of H3 on lysine 27; EZH, enhancer of zeste homolog; JMJD3, demethylase Jumonji domain-containing protein-3; UTX, ubiquitously transcribed tetratricopeptide repeat on chromosome X.

treatment with U0126 or Ly294002 induced SKM-1 cell cycle arrest in the G0/G1 phase and decreased the number of cells in the S phase, indicating that both inhibitors suppressed SKM-1 cell cycle progression (all P<0.05, Fig. 3C). Combined treatment with U0126 and Ly294002 exerted a more prominent effect on cell cycle arrest.

Furthermore, the results of EdU and colony formation assays revealed that treatment with U0126 or Ly294002 decreased SKM-1 cell proliferation, with cell proliferation being further inhibited by U0126 used in combination with Ly294002 (all P<0.05, Fig. 3D and E). Overall, these findings indicate that the MEK/ERK pathway inhibitor, U0126, and the PI3K/AKT pathway inhibitor, Ly294002, suppress SKM-1 cell cycle progression and proliferation.

Modulation of H3K27me3 methylases and de-methylases by MEK/ERK and PI3K/AKT pathway inhibitors. To further investigate the mechanisms of action of MEK/ERK and PI3K/AKT pathway inhibitors on SKM-1 cells, the present study examined whether these inhibitors can regulate the levels of H3K27me3 methylases and de-methylases. The results of western blot analysis revealed that treatment with U0126, the MEK/ERK pathway inhibitor, decreased the level of EZH2 (H3K27me3 methylase) and increased the level of JMJD3 (H3K27me3 de-methylase) in the SKM-1 cells (all P<0.05, Fig. 4). There were no significant changes in the levels of EZH1 (H3K27me3 methylase) or UTX (H3K27me3 de-methylase) following treatment with U0126 (all P>0.05). By contrast, treatment with Ly294002, the PI3K/AKT pathway inhibitor, decreased the level of EZH1 and increased the level of UTX in the SKM-1 cells (all P<0.05), with no significant changes in the EZH2 and JMJD3 levels (all P>0.05). Moreover, treatment with both U0126 and Ly294002 led to a more notable decrease in the EZH1 and EZH2 levels, and an increase in the JMJD3 and UTX levels compared to treatment with U0126 or Ly294002 alone.

Further analyses revealed that both inhibitors resulted in a significant decrease in the H3K27me3 protein levels, with the combined treatment exerting a more prominent inhibitory effect (all P<0.05, Fig. 4). Taken together, these findings suggest that MEK/ERK and PI3K/AKT pathway inhibitors can modulate the levels of H3K27me3 methylases and de-methylases, which may contribute to their inhibitory effects on SKM-1 cell proliferation and cycle progression.

EZH2 overexpression or JMJD3 knockdown partially abrogates the MEK/ERK pathway inhibitor-mediated effects on SKM-1 cells. Based on the aforementioned results, it was hypothesized that U0126 may affect the SKM-1 cell cycle and proliferation by modulating the H3K27me3 levels by down-regulating EZH2 and upregulating JMJD3 expression. To examine this hypothesis, SKM-1 cells were transfected with EZH2 overexpression plasmid or JMJD3 interference plasmids, followed by treatment with U0126. Western blot analysis confirmed the successful overexpression of EZH2 (P<0.05, Fig. 5A) and the knockdown of JMJD3 (P<0.05, Fig. 5B). Furthermore, EZH2 overexpression or JMJD3 knockdown led to an increase in the H3K27me3 protein levels (all P<0.05, Fig. 5A and B). The results of CCK-8 assay demonstrated that both EZH2 overexpression and JMJD3 knockdown enhanced SKM-1 cell viability following treatment with U0126 (all P<0.05, Fig. 5C). Flow cytometry revealed that EZH2 overexpression and JMJD3 knockdown counteracted the U0126-induced SKM-1 cell cycle arrest in the G0/G1 phase (all P<0.05, Fig. 5D). EdU and colony formation assays demonstrated that EZH2 overexpression or JMJD3 knockdown enhanced the proliferation of U0126-treated SKM-1 cells (all P<0.05, Fig. 5E and F). These findings suggest that EZH2 overexpression or JMJD3 knockdown can partially reverse the effects of MEK/ERK pathway inhibition on SKM-1 cell cycle in G0/G1 phase and proliferation.

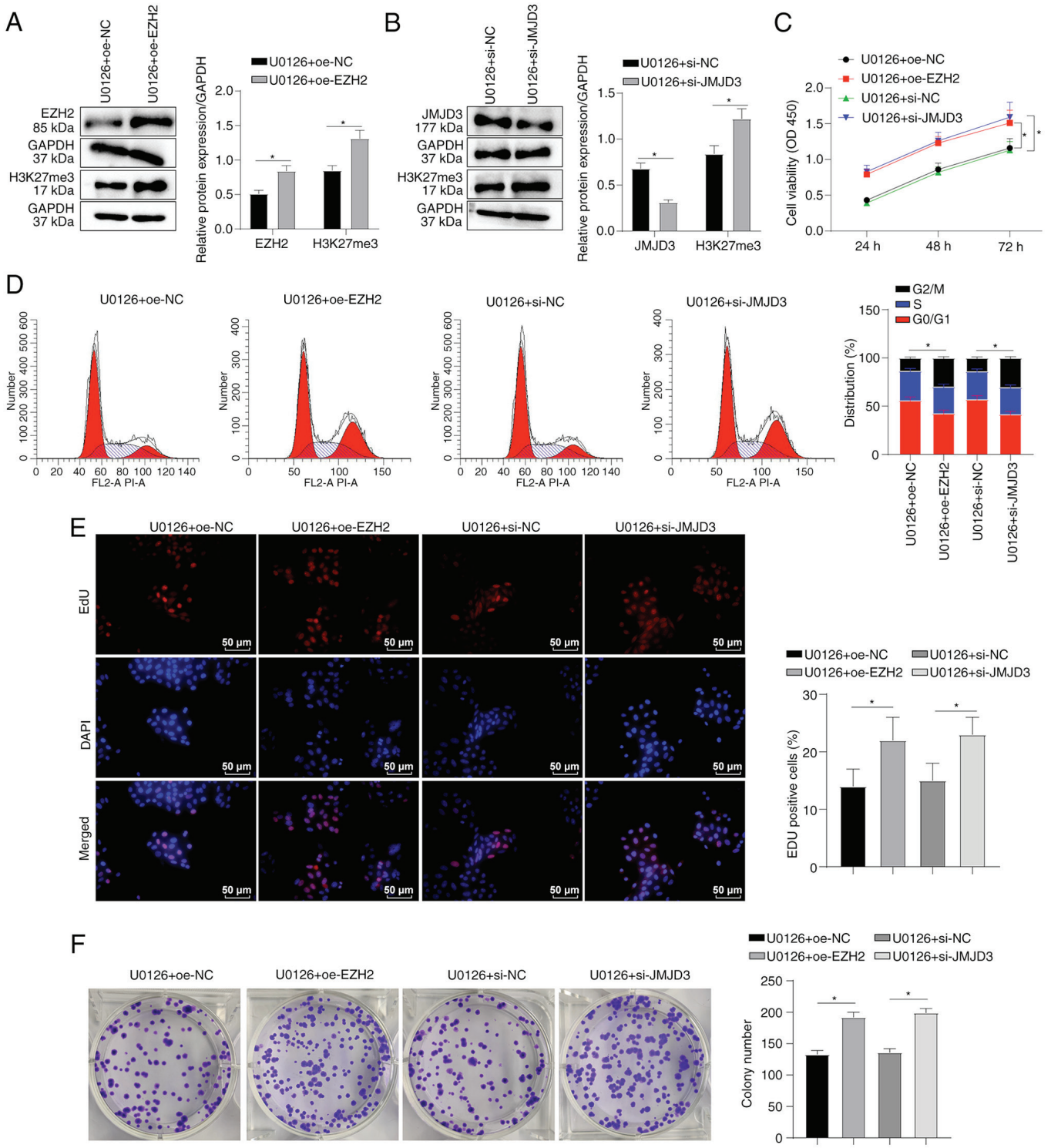

Figure 5. EZH2 overexpression or JMJD3 knockdown partially reverses the suppressive effects of MEK/ERK pathway inhibitors on SKM-1 cells. SKM-1 cells were transfected with EZH2 overexpression plasmid oe-EZH2 or JMJD3 interference plasmid si-JMJD3 for 48 h and then treated with the MEK/ERK inhibitor, U0126 (5 μM) for 48 h. (A and B) The protein levels of EZH2 or JMJD3 and H3K27me3 were measured using western blot analysis. (C) SKM-1 cell viability was assessed using CCK-8 assay. (D) SKM-1 cell cycle distribution was analyzed using flow cytometry. (E and F) SKM-1 cell proliferation was evaluated using EdU and colony formation assays. Each cell experiment was repeated three times. The results are expressed as the mean ± standard deviation. Pairwise comparison were analyzed using an independent t-test. *P<0.05. EZH2, enhancer of zeste homolog 2; JMJD3, demethylase Jumonji domain-containing protein-3; H3K27me3, trimethylation of H3 on lysine 27.

EZH1 overexpression or UTX knockdown partially annul the suppressive effects of PI3K/AKT pathway inhibitors on SKM-1 cells. In order to investigate the mechanisms through which the PI3K/AKT pathway inhibitor, Ly294002, affects SKM-1 cell cycle and proliferation, the present study examined the hypothesis that Ly294002 regulates EZH1 and UTX. To examine this hypothesis, SKM-1 cells were transfected with EZH1 overexpression plasmid or UTX interference plasmid, which respectively

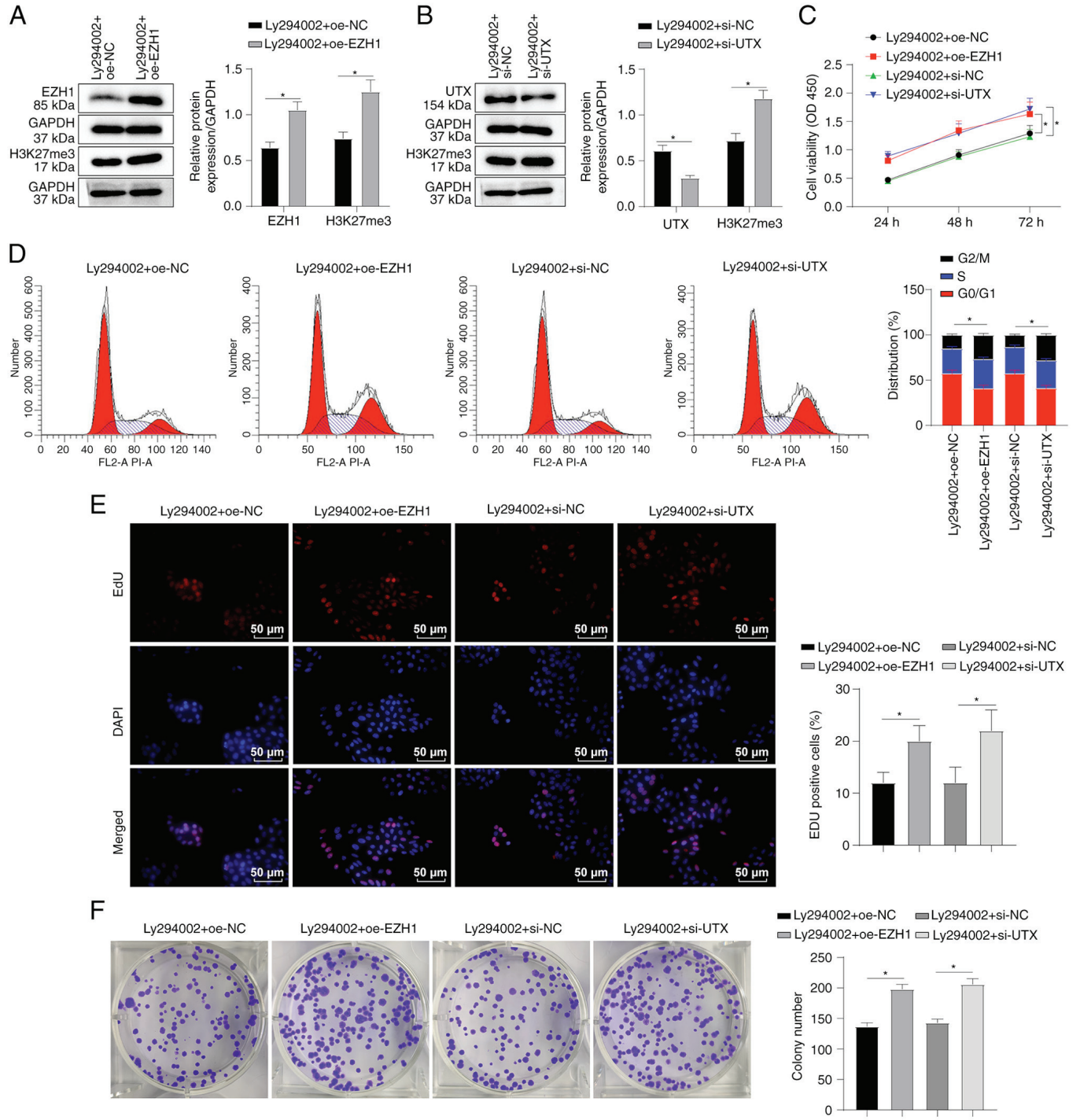

Figure 6. EZH1 overexpression or UTX knockdown partially annuls the suppressive effects of PI3K/AKT pathway inhibitors on SKM-1 cells. SKM-1 cells were transfected with EZH1 overexpression plasmid oe-EZH1 or UTX interference plasmid si-UTX for 48 h and then treated with the PI3K/AKT inhibitor, Ly294002 (5 μM) for 48 h. (A and B) The protein levels of EZH1 or UTX and H3K27me3 were measured using western blot analysis. (C) SKM-1 cell viability was assessed using CCK-8 assay. (D) SKM-1 cell cycle distribution was analyzed using flow cytometry. (E and F) SKM-1 cell proliferation was evaluated using EdU and colony formation assays. Each cell experiment was repeated three times. The results are expressed as the mean ± standard deviation. Pairwise comparison was analyzed using an independent t-test. *P<0.05. EZH1, enhancer of zeste homolog 1; H3K27me3, trimethylation of H3 on lysine 27; UTX, ubiquitously transcribed tetratricopeptide repeat on chromosome X.

overexpressed EZH1 or silenced UTX, and the cells were then treated with Ly294002. Western blot analysis confirmed the successful overexpression of EZH1 (P<0.05, Fig. 6A) and the knockdown of UTX (P<0.05, Fig. 6B). Additionally, it was found that EZH2 overexpression or UTX silencing led to an increase in the H3K27me3 protein level (all P<0.05, Fig. 6A and B). CCK-8 assay further revealed that both EZH1 overexpression and UTX knockdown enhanced the viability of the SKM-1 cells treated with Ly294002 (all P<0.05, Fig. 6C). Flow cytometry revealed that both EZH1 overexpression and UTX knockdown partially reversed the Ly294002-induced SKM-1 cell cycle arrest in the G0/G1 phase (all P<0.05, Fig. 6D). EdU and colony formation assays demonstrated that EZH1 overexpression or UTX knockdown increased the proliferation of Ly294002-treated

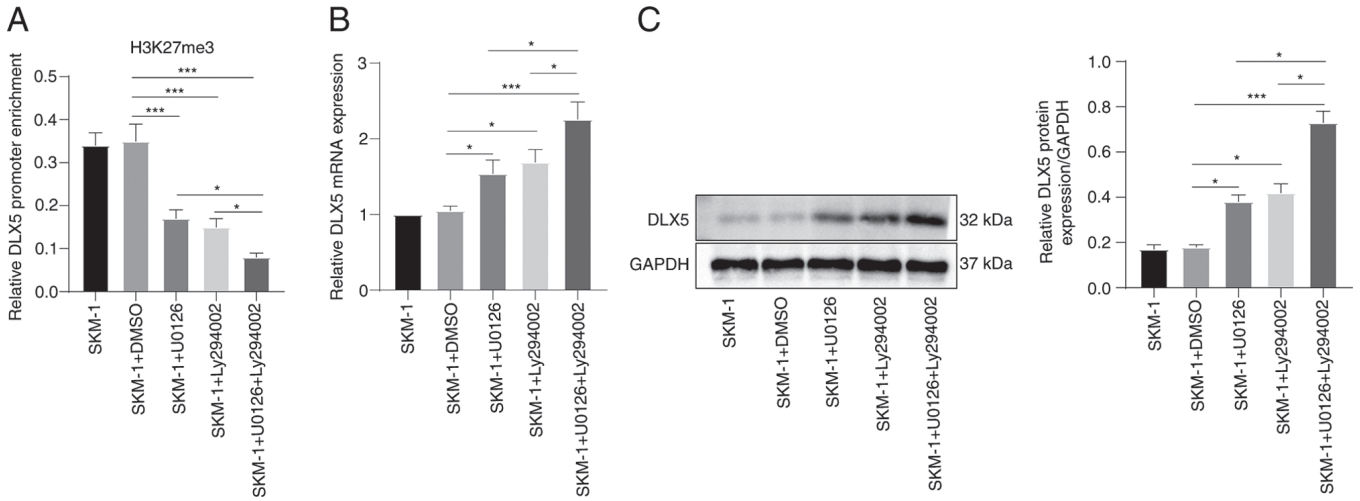

Figure 7. MEK/ERK and PI3K/AKT pathway inhibitors facilitate DLX5 transcription and expression by downregulating H3K27me3. (A) The level of DLX5 promoter region binding to H3K27me3 was examined using ChIP assay, and the graph shows RT-qPCR analysis of the binding content of the DLX5 promoter in DNA IP after ChIP, which is expressed as the content relative to control DNA input; the columns revealed the detection results of DLX5 ChIP primer 1, and the results were validated using DLX5 ChIP primer 2. The detection results of the two primers were similar. (B and C) DLX5 mRNA and protein levels in SKM-1 cells were measured using RT-qPCR and western blot analysis. Each cell experiment was repeated three times. The results are expressed as the mean ± standard deviation. Multi-group comparisons were performed using one-way ANOVA, followed by Tukey's multiple comparisons test. *P<0.05 and ***P<0.001. DLX5, distal-less homeobox 5; H3K27me3, trimethylation of H3 on lysine 27; RT-qPCR, reverse transcription-quantitative PCR.

SKM-1 cells (all P<0.05, Fig. 6E and F). Taken together, these findings suggest that EZH1 overexpression or UTX knockdown can partially overcome the inhibitory effects of Ly294002 on SKM-1 cell cycle and proliferation.

MEK/ERK and PI3K/AKT pathway inhibitors facilitate DLX5 transcription and expression by downregulating H3K27me3. As demonstrated above, U0126 and Ly294002 can modulate the expression of H3K27me3 methylases and de-methylases. ChIP analysis revealed that treatment with U0126 or Ly294002 decreased the enrichment of H3K27me3 in the DLX5 promoter region, and the reduction was more pronounced following combined treatment with U0126 and Ly294002 (all P<0.05, Fig. 7A). Furthermore, treatment with U0126 or Ly294002 alone increased the DLX5 levels, and their combination produced a more potent promoting effect (all P<0.05, Fig. 7B and C). Overall, these findings indicate that the MEK/ERK and PI3K/AKT pathway inhibitors, U0126 and Ly294002, respectively, can affect DLX5 transcription and expression by regulating the H3K227me3 levels through EZH2/JMJD3 and EZH1/UTX, respectively. Consequently, these pathways may play a crucial role in the progression of MDS and AML (Fig. 8).

Discussion

MDS is a severe hematological disorder that affects ~87,000 individuals worldwide each year. Unfortunately, in approximately one-third of patients, MDS eventually progresses to AML, which is associated with a poor prognosis (34). Previous research has indicated that MEK inhibitor can reverse resistance to bortezomib in patients with MDS, while PI3K inhibitor can enhance the apoptotic rates of SKM-1 cells (35,36). The pathogenesis of MDS involves DNA methylation and histone modifications, which are key pathological events (37). To the best of our knowledge, the present study is the first to demonstrated that MEK/ERK and PI3K/AKT pathway inhibitors modulate the transformation of MDS to AML by regulating DLX5 transcription and expression, and H3K27me3 levels via EZH2/JMJD3 and EZH1/UTX, respectively.

In the quest to identify effective treatments for MDS, numerous researchers have focused on the MEK/ERK and I3K/AKT signaling pathways. Wheeler *et al* (38) highlighted the potential of targeting the MEK/ERK pathway as a promising therapy for patients with MDS with mutations in splicing factors, while the activation of the PI3K/AKT pathway has been shown to play a role in the suppression of apoptosis in patients with high-risk MDS (39). The present study found that both patients with MDS and MDS-AML exhibited elevated levels of MEK/ERK and PI3K/AKT pathway activity, with patients with MDS-AML exhibiting particularly high levels; this was also observed in NHD13 mice, a commonly used animal model for MDS-AML (40). The inhibition of the PI3K/AKT pathway has been suggested as a possible treatment strategy for AML-MDS (13), and clinical trials have shown promise for MEK inhibition in patients with AML (41). In the present study, NHD13 mice were treated with U0126 or Ly294002, and the results were notable: Treatment resulted in a substantial increase in the number of RBCs, WBCs and PLTs, with decreased phosphorylation levels of ERK and AKT, the attenuated transformation of MDS into AML, and improved survival rates. The combined use of U0126 and Ly294002 was found to have a more prominent effect than the use of either inhibitor alone. In fact, MEK inhibition has been found to produce growth inhibitory and pro-apoptotic activities in AML preclinical models, particularly when used alongside other pathway inhibitors (42). The dual inhibition of PI3K/AKT and MEK pathways has also been found to be effective against RAS signaling-dependent tumors (43), and higher levels of SHIP1, a negative regulator of PI3K/AKT signaling, have been

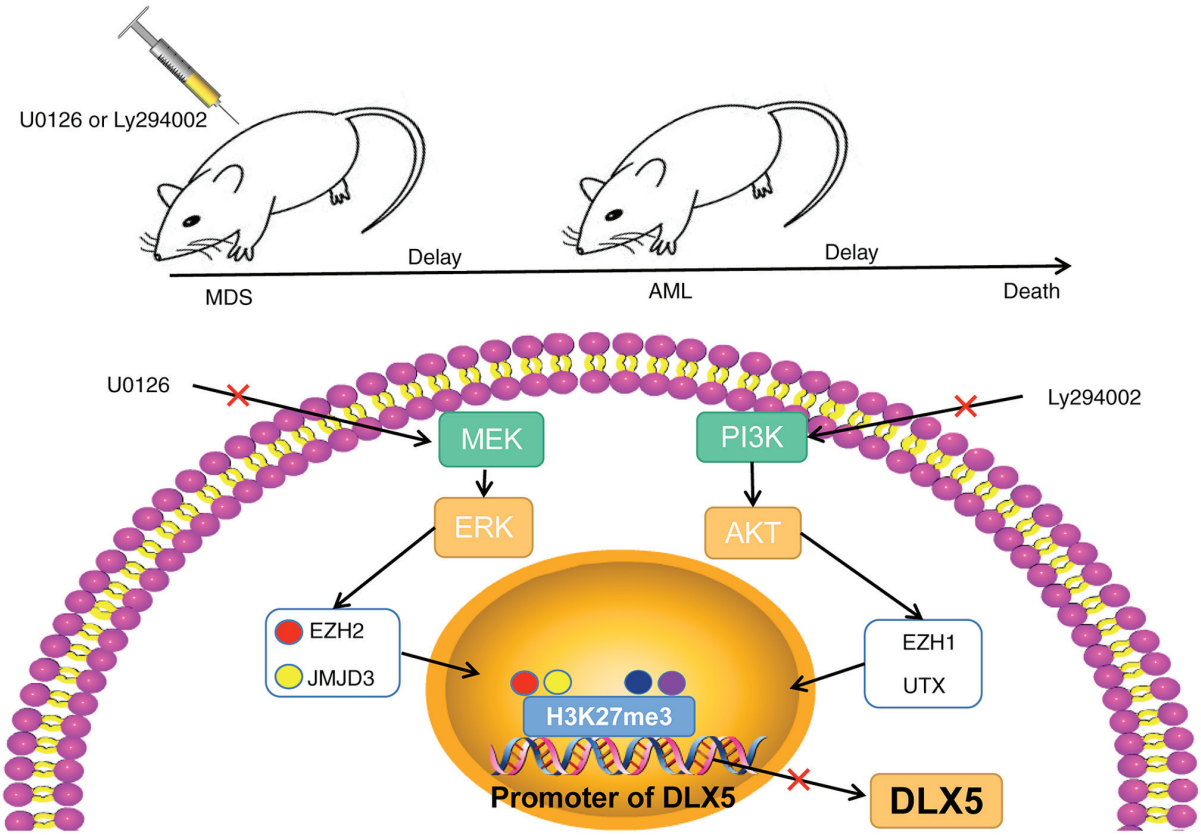

Figure 8. Schematic diagram of the role of the MEK/ERK and PI3K/AKT pathways in MDS-AML. The MEK/ERK and PI3K/AKT pathway inhibitors, U0126 and Ly294002, respectively, regulated te H3K27me3 level by mediating the levels of EZH2/JMJD3 and EZH1/UTX, thus affecting the transcription and expression of DLX5, and ultimately participating in the regulation of MDS and AML progression. MDS, myelodysplastic syndrome; AML, acute myeloid leukemia; EZH, enhancer of zeste homolog; H3K27me3, trimethylation of H3 on lysine 27; UTX, ubiquitously transcribed tetratricopeptide repeat on chromosome X; JMJD3, demethylase Jumonji domain-containing protein-3; JMJD3, demethylase Jumonji domain-containing protein-3.

found to be associated with a longer overall survival of patients with AML (44). Combined with these findings, the results of the present study suggest that targeting the MEK/ERK and PI3K/AKT pathways can effectively decelerate the progression of MDS to AML in mice. In addition, previous research has demonstrated that the inhibition of MEK/ERK pathway can impede the progression of AML cells from the G1 to the S phase, which is a crucial step in the cell cycle (45). Furthermore, Ly294002, a PI3K inhibitor, has been shown to function in synergy with SPAG6 shRNA lentivirus to induce the apoptosis of SKM-1 cells (36). In the present study, *in vitro* experiments using the SKM-1 cells also revealed that U0126 or Ly294002 were able to significantly suppress cell viability, promote cell cycle arrest in the G0/G1 phase, and decrease the cell proliferative ability, with combined treatment producing a more notable effect. Overall, these findings suggest that targeting the MEK/ERK and PI3K/AKT pathways may be an effective strategy with which to attenuate the progression of MDS into AML; this strategy may have potential as a treatment for patients with these conditions.

Previous studies have provided evidence that H3K27me3 levels play a role in the MDS transformation into AML (22), and the MEK/ERK and PI3K/AKT pathways are involved in the regulation of histone methylation and de-methylation (20,46). Specifically, the knockdown of EZH1 and EZH2 can reduce H3K27me3 (47), while JMJD3 and UTX can catalyze the de-methylation of H3K27me3 (48,49). The present study demonstrated that treatment with U0126 decreased the EZH2 levels and increased the JMJD3 levels in SKM-1 cells, while Ly294002 decreased the EZH1 levels and augmented the UTX levels. Moreover, combined treatment with U0126 and Ly294002 led to the downregulation of EZH1 and EZH2, and the upregulation of JMJD3 and UTX expression. Furthermore, treatment with either U0126 or Ly294002 suppressed the protein level of H3K27me3, and combined treatment had a more prominent inhibitory effect. In cancer cells, a high EZH2 expression can increase the H3K27me3 levels by activating the MEK/ERK pathway (50), and EZH2 can manipulate the PI3K pathway in an H3K27me3-dependent manner (51). Therefore, inhibitors of the MEK/ERK and PI3K/AKT pathway can modulate the expression levels of H3K27me3 methylases and de-methylases and suppress the downstream protein level of H3K27me3. Herein, it was observed that the combined use of the MEK/ERK and PI3K/AKT inhibitors had more significant regulatory effects on EZH1, EZH2, JMJD3, UTX and H3K27me. Studies have demonstrated that the activation of the PI3K/AKT pathway can inhibit the activation of the MEK/ERK pathway, while the inhibition of the MEK/ERK pathway can lead to the activation of the PI3K/AKT pathway (52,53). There may be some competitive association between the PI3K/AKT pathway and the MEK/ERK pathway, where there may be signal interference and interaction between them (54,55). In some tumor studies, it has been observed that the simultaneous inhibition of the MEK/ERK and PI3K/AKT pathways

has synergistic effects. For example, in multiple myeloma, U0126 and Ly294002 have been shown to exert synergistic effects (56). In liver cancer, U0126 and Ly294002 can synergistically inhibit cell proliferation and promote cell apoptosis (57). Therefore, U0126 and Ly294002 may have a synergistic effect, while inhibiting the MEK/ERK and PI3K/AKT pathways can further downregulate EZH1, EZH2 and H3K27me3, and upregulate the protein levels of JMJD and UTX compared to the use of a single inhibitor. Moreover, DLX5 methylation has been shown to participate in leukemogenesis via the PI3K/AKT pathway (21). The present study revealed that treatment with either U0126 or Ly294002 suppressed the H3K27me3 protein level, inhibited H3K27me3 expression in the DLX3 promoter region, and enhanced the DLX5 mRNA and protein levels. Previous research has indicated that DLX5 transcription and expression are regulated by H3K27me3 regulation, and are associated with MDS progression (22). Therefore, inhibitors of the MEK/ERK and PI3K/AKT pathways, such as U0126 and Ly294002, may modulate DLX5 transcription and expression through the regulation of H3K27me3.

The overexpression of EZH2 is frequently observed in high-risk MDS and AML (58), while JMJD3 has been shown to have oncosuppressor activity in AML (59). The present study revealed that EZH2 overexpression or JMJD3 knockdown resulted in increased H3K27me3 protein levels, SKM-1 cell viability and proliferation, and abolished cell cycle arrest following treatment with U0126. EZH1 plays a significant role in EZH2-inadequate MDS (60), while UTX mutation can potentiate MDS and AML (61). In the presents study, EZH1 overexpression or silencing UTX increased the H3K27me3 protein levels, enhanced SKM-1 cell viability and proliferation, and counteracted cell cycle arrest following treatment with Ly294002. The MER/ERK/Elk-1 pathway leads to EZH2 overexpression in breast cancer cell lines (62), and mTet1 upregulates JMJD3 to decrease H3K27me3, thus suppressing the MEK/ERK pathway in male germline stem cells (50). Additionally, EZH1 knockdown enhances the sensitivity of multiple myeloma cells to AKT inhibition (19), while UTX increases PTEN expression to downregulate p-AKT and p-mTOR in somatic cells (63). Taken together, the overexpression of EZH2 and EZH1 or the knockdown of JMJD3 or UTX can partially counteract the effects of U0126 or Ly294002 on SKM-1 cell cycle and proliferation.

In conclusion, the present study highlights the potential of MEK/ERK and PI3K/AKT pathway inhibitors as therapeutic targets for MDS and AML. By modulating the EZH2/JMJD3 and EZH1/UTX levels, these inhibitors can affect H3K27me3 and ultimately, DLX5 transcription and expression. However, the present study is limited by the small sample size in clinical and animal experiments, the lack of result validation in animal experiments, and the need to explore other regulatory mechanisms of DLX5, such as the influence of the pathway inhibitors on H3K9me1/2. Further studies are thus warranted to address these gaps and fully elucidate the functional mechanisms of DLX5 in the MDS-AML transformation.

Acknowledgements

Not applicable.

Funding

The present study was funded by The Shanxi Province Applied Basic Research: Natural Science Foundation (grant no. 201801D121330), which aims to investigate the association between molecular biology abnormalities based on epigenetic modifiers and mRNA precursor splicing factors and the prognosis of myelodysplastic syndromes.

Availability of data and materials

The datasets used and/or analyzed during the current study are available from the corresponding author on reasonable request.

Authors' contributions

YM was responsible for ensuring the integrity of the entire study and contributed to the editing and reviewing of the manuscript. ZZ and YM contributed to the conception and design of the study concepts, as well as in the development of intellectual content and literature research. FR contributed to the clinical studies and statistical analysis. XC and YZ contributed to the experiments. XC contributed to data acquisition, and YZ contributed to data analysis. YM and ZZ confirm the authenticity of all the raw data. All authors have read and approved the final manuscript.

Ethics approval and consent to participate

The present study was conducted in accordance with the guidelines of the Ethics Committee of Second Hospital of Shanxi Medical University (Taiyuan, China). Informed consent was obtained from all participants before sampling (Approval no. 2020-YX-056). The animal experiments were performed with the aim of minimizing the number of animals used and reducing their suffering (Approval no. 2020-K52). Significant effort was made in animal experiments to minimize the number of animals used and their suffering.

Patient consent for publication

Not applicable.

Competing interests

The authors declare that they have no competing interests.

References

1. Hasserjian RP: Myelodysplastic syndrome updated. Pathobiology 86: 7-13, 2019.
2. Haferlach T: The molecular pathology of myelodysplastic syndrome. Pathobiology 86: 24-29, 2019.
3. Yan X, Lai B, Zhou X, Yang S, Ge Q, Zhou M, Shi C, Xu Z and Ouyang G: The differential expression of CD47 may be related to the pathogenesis from myelodysplastic syndromes to acute myeloid leukemia. Front Oncol 12: 872999, 2022.
4. Menssen AJ and Walter MJ: Genetics of progression from MDS to secondary leukemia. Blood 136: 50-60, 2020.
5. Rankin EB, Narla A, Park JK, Lin S and Sakamoto KM: Biology of the bone marrow microenvironment and myelodysplastic syndromes. Mol Genet Metab 116: 24-28, 2015.

6. Liu W, Teodorescu P, Halene S and Ghiaur G: The coming of age of preclinical models of MDS. Front Oncol 12: 815037, 2022.
7. Venney D, Mohd-Sarip A and Mills KI: The impact of epigenetic modifications in myeloid malignancies. Int J Mol Sci 22: 5013, 2021.
8. Shukron O, Vainstein V, Kündgen A, Germing U and Agur Z: Analyzing transformation of myelodysplastic syndrome to secondary acute myeloid leukemia using a large patient database. Am J Hematol 87: 853-860, 2012.
9. Zhang Z, Richmond A and Yan C: Immunomodulatory properties of PI3K/AKT/mTOR and MAPK/MEK/ERK inhibition augment response to immune checkpoint blockade in melanoma and triple-negative breast cancer. Int J Mol Sci 23: 7353, 2022.
10. Fu NJ, Xi RY, Shi XK, Li RZ, Zhang ZH, Li LY, Zhang GL and Wang F: Hexachlorophene, a selective SHP2 inhibitor, suppresses proliferation and metastasis of KRAS-mutant NSCLC cells by inhibiting RAS/MEK/ERK and PI3K/AKT signaling pathways. Toxicol Appl Pharmacol 441: 115988, 2022.
11. Peng M, Fan S, Li J, Zhou X, Liao Q, Tang F and Liu W: Programmed death-ligand 1 signaling and expression are reversible by lycopene via PI3K/AKT and Raf/MEK/ERK pathways in tongue squamous cell carcinoma. Genes Nutr 17: 3, 2022.
12. Zebisch A, Czernilofsky AP, Keri G, Smigelskaite J, Sill H and Troppmair J: Signaling through RAS-RAF-MEK-ERK: From basics to bedside. Curr Med Chem 14: 601-623, 2007.
13. Liang S, Zhou X, Cai D, Rodrigues-Lima F, Chi J and Wang L: Network pharmacology and experimental validation reveal the effects of chidamide combined with aspirin on acute myeloid leukemia-myelodysplastic syndrome cells through PI3K/AKT pathway. Front Cell Dev Biol 9: 685954, 2021.
14. Akutagawa J, Huang TQ, Epstein I, Chang T, Quirindongo-Crespo M, Cottonham CL, Dail M, Slusher BS, Friedman LS, Sampath D and Braun BS: Targeting the PI3K/Akt pathway in murine MDS/MPN driven by hyperactive Ras. Leukemia 30: 1335-1343, 2016.
15. Chung E, Hsu CL and Kondo M: Constitutive MAP kinase activation in hematopoietic stem cells induces a myeloproliferative disorder. PLoS One 6: e28350, 2011.
16. Gonzalez-Lugo JD, Chakraborty S, Verma A and Shastri A: The evolution of epigenetic therapy in myelodysplastic syndromes and acute myeloid leukemia. Semin Hematol 58: 56-65, 2021.
17. Hojfeldt JW, Agger K and Helin K: Histone lysine demethylases as targets for anticancer therapy. Nat Rev Drug Discov 12: 917-930, 2013.
18. Ruan XF, Li YJ, Ju CW, Shen Y, Lei W, Chen C, Li Y, Yu H, Liu YT, Kim IM, *et al*: Exosomes from Suxiao Jiuxin pill-treated cardiac mesenchymal stem cells decrease H3K27 demethylase UTX expression in mouse cardiomyocytes in vitro. Acta Pharmacol Sin 39: 579-586, 2018.
19. Rizk M, Rizq O, Oshima M, Nakajima-Takagi Y, Koide S, Saraya A, Isshiki Y, Chiba T, Yamazaki S, Ma A, *et al*: Akt inhibition synergizes with polycomb repressive complex 2 inhibition in the treatment of multiple myeloma. Cancer Sci 110: 3695-3707, 2019.
20. Ferraro A, Mourtzoukou D, Kosmidou V, Avlonitis S, Kontogeorgos G, Zografos G and Pintzas A: EZH2 is regulated by ERK/AKT and targets integrin alpha2 gene to control epithelial-mesenchymal transition and anoikis in colon cancer cells. Int J Biochem Cell Biol 45: 243-254, 2013.
21. Zhang TJ, Xu ZJ, Gu Y, Wen XM, Ma JC, Zhang W, Deng ZQ, Leng JY, Qian J, Lin J and Zhou JD: Identification and validation of prognosis-related DLX5 methylation as an epigenetic driver in myeloid neoplasms. Clin Transl Med 10: e29, 2020.
22. Zheng Z, Li L, Li G, Zhang Y, Dong C, Ren F, Chen W and Ma Y: EZH2/EHMT2 histone methyltransferases inhibit the transcription of DLX5 and promote the transformation of myelodysplastic syndrome to acute myeloid leukemia. Front Cell Dev Biol 9: 619795, 2021.
23. Arber DA, Orazi A, Hasserjian R, Thiele J, Borowitz MJ, Le Beau MM, Bloomfield CD, Cazzola M and Vardiman JW: The 2016 revision to the World Health Organization classification of myeloid neoplasms and acute leukemia. Blood 127: 2391-2405, 2016.
24. You Y, Niu Y, Zhang J, Huang S, Ding P, Sun F and Wang X: U0126: Not only a MAPK kinase inhibitor. Front Pharmacol 13: 927083, 2022.
25. Xu CN, Kong LH, Ding P, Liu Y, Fan ZG, Gao EH, Yang J and Yang LF: Melatonin ameliorates pressure overload-induced cardiac hypertrophy by attenuating Atg5-dependent autophagy and activating the Akt/mTOR pathway. Biochim Biophys Acta Mol Basis Dis 1866: 165848, 2020.
26. Guirguis AA, Slape CI, Failla LM, Saw J, Tremblay CS, Powell DR, Rossello F, Wei A, Strasser A and Curtis DJ: PUMA promotes apoptosis of hematopoietic progenitors driving leukemic progression in a mouse model of myelodysplasia. Cell Death Differ 23: 1049-1059, 2016.
27. Estey E, Hasserjian RP and Döhner H: Distinguishing AML from MDS: A fixed blast percentage may no longer be optimal. Blood 139: 323-332, 2022.
28. Zatroch KK, Knight CG, Reimer JN and Pang DS: Refinement of intraperitoneal injection of sodium pentobarbital for euthanasia in laboratory rats (Rattus norvegicus). BMC Vet Res 13: 60, 2017.
29. Geng Y, Wu W, Zhou L, Li J, Geng Y and Yang Y: Synergistic effects of LY294002 and ABT199 on the cell cycle in K562, HL60 and KG1a cells. Oncol Rep 45: 97, 2021.
30. Wang C, Wang K, Li SF, Song SJ, Du Y, Niu RW, Qian XW, Peng XQ and Chen FH: 4-Amino-2-trifluoromethyl-phenyl retinate induced differentiation of human myelodysplastic syndromes SKM-1 cell lines by up-regulating DDX23. Biomed Pharmacother 123: 109736, 2020.
31. Zhou W, Xu S, Ying Y, Zhou R and Chen X: Resveratrol suppresses growth and migration of myelodysplastic cells by inhibiting the expression of elevated cyclin D1 (CCND1). DNA Cell Biol 36: 966-975, 2017.
32. Dagdemir A, Durif J, Ngollo M, Bignon YJ and Bernard-Gallon D: Histone lysine trimethylation or acetylation can be modulated by phytoestrogen, estrogen or anti-HDAC in breast cancer cell lines. Epigenomics 5: 51-63, 2013.
33. Livak KJ and Schmittgen TD: Analysis of relative gene expression data using real-time quantitative PCR and the 2(-Delta Delta C(T)) method. Methods 25: 402-408, 2001.
34. Trivedi G, Inoue D and Zhang L: Targeting low-risk myelodysplastic syndrome with novel therapeutic strategies. Trends Mol Med 27: 990-999, 2021.
35. Yue Y, Wang Y, He Y, Yang S, Chen Z, Wang Y, Xing S, Shen C, Amin HM, Wu D and Song YH: Reversal of bortezomib resistance in myelodysplastic syndrome cells by MAPK inhibitors. PLoS One 9: e90992, 2014.
36. Yin J, Li X, Zhang Z, Luo X, Wang L and Liu L: SPAG6 silencing induces apoptosis in the myelodysplastic syndrome cell line SKM-1 via the PTEN/PI3K/AKT signaling pathway *in vitro* and *in vivo*. Int J Oncol 53: 297-306, 2018.
37. Lee P, Yim R, Yung Y, Chu HT, Yip PK and Gill H: Molecular targeted therapy and immunotherapy for myelodysplastic syndrome. Int J Mol Sci 22: 10232, 2021.
38. Wheeler EC, Vora S, Mayer D, Kotini AG, Olszewska M, Park SS, Guccione E, Teruya-Feldstein J, Silverman L, Sunahara RK, *et al*: Integrative RNA-omics discovers GNAS alternative splicing as a phenotypic driver of splicing factor-mutant neoplasms. Cancer Discov 12: 836-855, 2022.
39. Lin S, Li J, Zhou W, Qian W, Wang B and Chen Z: BIIB021, an Hsp90 inhibitor, effectively kills a myelodysplastic syndrome cell line via the activation of caspases and inhibition of PI3K/Akt and NF-κB pathway proteins. Exp Ther Med 7: 1539-1544, 2014.
40. Lin YW, Slape C, Zhang Z and Aplan PD: NUP98-HOXD13 transgenic mice develop a highly penetrant, severe myelodysplastic syndrome that progresses to acute leukemia. Blood 106: 287-295, 2005.
41. Maiti A, Naqvi K, Kadia TM, Borthakur G, Takahashi K, Bose P, Daver NG, Patel A, Alvarado Y, Ohanian M, *et al*: Phase II trial of MEK inhibitor binimetinib (MEK162) in RAS-mutant acute myeloid leukemia. Clin Lymphoma Myeloma Leuk 19: 142-148. e1, 2019.
42. Ricciardi MR, Scerpa MC, Bergamo P, Ciuffreda L, Petrucci MT, Chiaretti S, Tavolaro S, Mascolo MG, Abrams SL, Steelman LS, *et al*: Therapeutic potential of MEK inhibition in acute myelogenous leukemia: Rationale for 'vertical' and 'lateral' combination strategies. J Mol Med (Berl) 90: 1133-1144, 2012.
43. Ragon BK, Odenike O, Baer MR, Stock W, Borthakur G, Patel K, Han L, Chen H, Ma H, Joseph L, *et al*: Oral MEK 1/2 inhibitor trametinib in combination with AKT inhibitor GSK2141795 in patients with acute myeloid leukemia with RAS mutations: A phase II study. Clin Lymphoma Myeloma Leuk 19: 431-440.e13, 2019.
44. Täger M, Horn S, Latuske E, Ehm P, Schaks M, Nalaskowski M, Fehse B, Fiedler W, Stocking C, Wellbrock J and Jücker M: SHIP1, but not an AML-derived SHIP1 mutant, suppresses myeloid leukemia growth in a xenotransplantation mouse model. Gene Ther 24: 749-753, 2017.

45. Lin L, Que Y, Lu P, Li H, Xiao M, Zhu X and Li D: Chidamide inhibits acute myeloid leukemia cell proliferation by lncRNA VPS9D1-AS1 downregulation via MEK/ERK signaling pathway. Front Pharmacol 11: 569651, 2020.
46. Riquelme E, Behrens C, Lin HY, Simon G, Papadimitrakopoulou V, Izzo J, Moran C, Kalhor N, Lee JJ, Minna JD and Wistuba II: Modulation of EZH2 expression by MEK-ERK or PI3K-AKT signaling in lung cancer is dictated by different KRAS oncogene mutations. Cancer Res 76: 675-685, 2016.
47. Yamagishi M, Hori M, Fujikawa D, Ohsugi T, Honma D, Adachi N, Katano H, Hishima T, Kobayashi S, Nakano K, *et al*: Targeting excessive EZH1 and EZH2 activities for abnormal histone methylation and transcription network in malignant lymphomas. Cell Rep 29: 2321-2337.e7, 2019.
48. Rejlova K, Musilova A, Kramarzova KS, Zaliova M, Fiser K, Alberich-Jorda M, Trka J and Starkova J: Low HOX gene expression in PML-RARα-positive leukemia results from suppressed histone demethylation. Epigenetics 13: 73-84, 2018.
49. Agger K, Cloos PA, Christensen J, Pasini D, Rose S, Rappsilber J, Issaeva I, Canaani E, Salcini AE and Helin K: UTX and JMJD3 are histone H3K27 demethylases involved in HOX gene regulation and development. Nature 449: 731-734, 2007.
50. Zheng L, Zhai Y, Li N, Ma F, Zhu H, Du X, Li G and Hua J: The modification of Tet1 in male germline stem cells and interact with PCNA, HDAC1 to promote their self-renewal and proliferation. Sci Rep 6: 37414, 2016.
51. Kosalai ST, Morsy MHA, Papakonstantinou N, Mansouri L, Stavroyianni N, Kanduri C, Stamatopoulos K, Rosenquist R and Kanduri M: EZH2 upregulates the PI3K/AKT pathway through IGF1R and MYC in clinically aggressive chronic lymphocytic leukaemia. Epigenetics 14: 1125-1140, 2019.
52. Zitzmann K, Rüden J, Brand S, Göke B, Lichtl J, Spöttl G and Auernhammer CJ: Compensatory activation of Akt in response to mTOR and Raf inhibitors-a rationale for dual-targeted therapy approaches in neuroendocrine tumor disease. Cancer Lett 295: 100-109, 2010.
53. Turke AB, Song Y, Costa C, Cook R, Arteaga CL, Asara JM and Engelman JA: MEK inhibition leads to PI3K/AKT activation by relieving a negative feedback on ERBB receptors. Cancer Res 72: 3228-3237, 2012.
54. Wu YL, Maachani UB, Schweitzer M, Singh R, Wang M, Chang R and Souweidane MM: Dual inhibition of PI3K/AKT and MEK/ERK pathways induces synergistic antitumor effects in diffuse intrinsic pontine glioma cells. Transl Oncol 10: 221-228, 2017.
55. Cao Z, Liao Q, Su M, Huang K, Jin J and Cao D: AKT and ERK dual inhibitors: The way forward? Cancer Lett 459: 30-40, 2019.
56. Ramakrishnan V, Kimlinger T, Haug J, Painuly U, Wellik L, Halling T, Rajkumar SV and Kumar S: Anti-myeloma activity of Akt inhibition is linked to the activation status of PI3K/Akt and MEK/ERK pathway. PLoS One 7: e50005, 2012.
57. Liu L, Chen J, Cao M, Wang J and Wang S: NO donor inhibits proliferation and induces apoptosis by targeting PI3K/AKT/mTOR and MEK/ERK pathways in hepatocellular carcinoma cells. Cancer Chemother Pharmacol 84: 1303-1314, 2019.
58. Xu F, Li X, Wu L, Zhang Q, Yang R, Yang Y, Zhang Z, He Q and Chang C: Overexpression of the EZH2, RING1 and BMI1 genes is common in myelodysplastic syndromes: Relation to adverse epigenetic alteration and poor prognostic scoring. Ann Hematol 90: 643-653, 2011.
59. Yu SH, Zhu KY, Chen J, Liu XZ, Xu PF, Zhang W, Yan L, Guo HZ and Zhu J: JMJD3 facilitates C/EBPβ-centered transcriptional program to exert oncorepressor activity in AML. Nat Commun 9: 3369, 2018.
60. Mochizuki-Kashio M, Aoyama K, Sashida G, Oshima M, Tomioka T, Muto T, Wang C and Iwama A: Ezh2 loss in hematopoietic stem cells predisposes mice to develop heterogeneous malignancies in an Ezh1-dependent manner. Blood 126: 1172-1183, 2015.
61. Wu B, Pan X, Chen X, Chen M, Shi K, Xu J, Zheng J, Niu T, Chen C, Shuai X and Liu Y: Epigenetic drug library screening identified an LSD1 inhibitor to target UTX-deficient cells for differentiation therapy. Signal Transduct Target Ther 4: 11, 2019.
62. Fujii S, Tokita K, Wada N, Ito K, Yamauchi C, Ito Y and Ochiai A: MEK-ERK pathway regulates EZH2 overexpression in association with aggressive breast cancer subtypes. Oncogene 30: 4118-4128, 2011.
63. Jiang Q, Huang X, Hu X, Shan Z, Wu Y, Wu G and Lei L: Histone demethylase KDM6A promotes somatic cell reprogramming by epigenetically regulating the PTEN and IL-6 signal pathways. Stem Cells 38: 960-972, 2020.